



Published in final edited form as:

Invest Ophthalmol Vis Sci. 2008 September ; 49(9): 3747–3757. doi:10.1167/iovs.07-1493.

Peripheral refraction in normal infant rhesus monkeys

Li-Fang Hung^{1,2}, Ramkumar Ramamirtham^{1,2,3}, Juan Huang^{1,2}, Ying Qiao-Grider^{1,2}, and Earl L. Smith III^{1,2}

¹College of Optometry, University of Houston, Houston, TX 77204-2020, USA

²Vision CRC, Sydney NSW 2052, Australia

Abstract

Purpose—To characterize peripheral refractions in infant monkeys.

Methods—Cross-sectional data for horizontal refractions were obtained from 58 normal rhesus monkeys at 3 weeks of age. Longitudinal data were obtained for both the vertical and horizontal meridians from 17 monkeys. Refractive errors were measured by retinoscopy along the pupillary axis and at eccentricities of 15, 30, and 45 degrees. Axial dimensions and corneal power were measured by ultrasonography and keratometry, respectively.

Results—In infant monkeys, the degree of radial astigmatism increased symmetrically with eccentricity in all meridians. There were, however, initial nasal-temporal and superior-inferior asymmetries in the spherical-equivalent refractive errors. Specifically, the refractions in the temporal and superior fields were similar to the central ametropia, but the refractions in the nasal and inferior fields were more myopic than the central ametropia and the relative nasal field myopia increased with the degree of central hyperopia. With age, the degree of radial astigmatism decreased in all meridians and the refractions became more symmetrical along both the horizontal and vertical meridians; small degrees of relative myopia were evident in all fields.

Conclusions—As in adult humans, refractive error varied as a function of eccentricity in infant monkeys and the pattern of peripheral refraction varied with the central refractive error. With age, emmetropization occurred for both central and peripheral refractive errors resulting in similar refractions across the central 45 degrees of the visual field, which may reflect the actions of vision-dependent, growth-control mechanisms operating over a wide area of the posterior globe.

Keywords

hyperopia; radial astigmatism; refractive error; emmetropization

INTRODUCTION

In humans, refractive error varies as a function of eccentricity. In addition to the increase in radial astigmatism with eccentricity, spherical-equivalent refractive errors in the periphery can often be very different from those measured at the fovea.^{1–11} Interestingly, the pattern of peripheral refractive errors varies with foveal refractive error. On average, both children and adults who exhibit myopia at the fovea typically demonstrate less myopia or more hyperopia in the periphery^{6,10–13} and the magnitude of this relative peripheral hyperopia increases with

Corresponding author: Earl L. Smith III, University of Houston, College of Optometry, 505 J Armistead Bldg, Houston, TX 77204-2020, Tel: 713-743-1946; Fax: 713-743-2053; e-mail: esmith@uh.edu.

³Present address: Alcon Laboratories, Inc, Fort Worth, TX 76134, USA

Proprietary interest: None

the degree of axial myopia.^{11,14} In contrast, hyperopic individuals typically exhibit less hyperopia or more myopia in the periphery and emmetropes, on average, have the smallest peripheral refractive errors.^{6,8,10,15}

Understanding the relationship between central and peripheral refractive errors is important because the pattern of peripheral refractive errors has been implicated in the genesis of common central refractive errors. For example, emmetropic young adults who show compound hyperopic astigmatism in the periphery are more likely to exhibit myopic shifts in central refractive error during pilot training than individuals who exhibit myopic peripheral refractive errors.¹⁶ Similarly, children with more prolate shaped posterior segments or relative hyperopia in the periphery are more likely to develop central myopia or to exhibit faster myopic progression than children with oblate shaped eyes and relative myopia in the periphery.^{12, 13,15-17} These observations are in agreement with the hypothesis that peripheral hyperopia provides a visual signal for axial elongation.¹⁸⁻²¹ This idea is attractive because accommodation is typically postured to optimize central vision. As a consequence, for a given fixation plane the defocus associated with any differences between central and peripheral refractions would be relatively constant over time, a key factor in determining whether a myopiagenic stimulus produces myopia.²²⁻²⁶ Similarly, it is possible that the relative peripheral myopia found in hyperopic children¹⁵ may retard axial elongation and promote the development of abnormal amounts of hyperopia.

At first glance, it might not seem feasible that peripheral defocus could overshadow the effects of central vision because the density for most retinal neurons is much greater in the central retina. However, as Wallman and Winawer²¹ have argued, the total area of the central retina is quite small and because the area of the peripheral retina is so much larger, the absolute number of neurons in the retinal periphery greatly exceeds the number of central neurons. The key point is that, depending on how central and peripheral signals are pooled, the refractive state at the fovea may not reflect the overall balance of visual signals for eye growth.

Although it has generally been assumed that visual signals from the fovea direct refractive development, experiments in monkeys demonstrate that peripheral vision can dominate central refractive development. For example, eliminating visual signals from the fovea does not interfere with emmetropization in infant monkeys nor does it prevent the axial myopia produced by form deprivation or the compensating changes in axial growth produced by experimentally imposed refractive errors (Smith et al. *IOVS* 2007; ARVO E-Abstract 1533).^{18,20} Moreover, selectively imposing hyperopic defocus or form deprivation in the periphery produces central axial myopia in infant monkeys (Smith et al. *IOVS* 2007; ARVO E-Abstract 1533).¹⁸ Thus, peripheral vision can have a substantial impact on normal emmetropization and the development of anomalous, vision-induced refractive errors.

The manner in which the vision-dependent mechanisms integrate visual information across the retina is important for understanding the potential impact of peripheral refractive errors. In this respect, studies in birds²⁷⁻²⁹ and tree shrews³⁰ have demonstrated that eye growth is regulated by local retinal mechanisms that integrate visual signals over spatially restricted areas across the retina and that alterations in peripheral vision can have a significant impact on eye shape and potentially on axial length for the central retina. In fact it has been argued that the lower-field myopia observed in many species represents a compensating, emmetropizing response to asymmetries in viewing distance across the visual field (in essence, asymmetries in the effective peripheral refractive error).³¹⁻³³

Thus, peripheral refractive errors may contribute to the development of common axial refractive errors, serve as a sensitive predictive indicator for those individuals who are most likely to develop myopia, influence ocular shape via vision-dependent mechanisms, and

potentially be manipulated via optical treatment strategies to control central refractive development. In this respect, it is possible that the pattern of peripheral refraction is inherited and that genetic factors that influence corneal, crystalline lens and/or posterior globe shape predispose some eyes toward central myopia. It is unfortunate that relatively little is known about the pattern of peripheral refractive errors in infants. It is well established that central refractive errors can change dramatically early in life and that the changes in central refraction reflect alterations in the eye's optical and axial dimensions that are also likely to affect peripheral refraction, i.e., it is likely that there are also substantial changes in peripheral refraction early in life. In addition, it is possible that the pattern of peripheral refractive errors has an influence on the course of emmetropization. Therefore, the purpose of this study was to characterize peripheral refractions in normal infant rhesus monkeys. Some of these results have been presented in abstract form (Hung et al., International Myopia Conference in Singapore 2007: Abstract SO52).

MATERIALS AND METHODS

Subjects

The subjects were 58 infant rhesus monkeys (*Macaca mulatta*) that were obtained at 1 to 3 weeks of age and housed in our primate nursery that was maintained on a 12-hour light / 12-hour dark lighting cycle.³⁴ All of the rearing and experimental procedures were reviewed and approved by the University of Houston's Institutional Animal Care and Use Committee and were in compliance with the ARVO Statement for the Use of Animals in Ophthalmic and Vision Research.

Cross-sectional data on axial dimensions, corneal curvature, and central and peripheral refractive errors were obtained from all 58 monkeys prior to the onset of any experimental manipulation at about 3 weeks of age (24.2 ± 3.7 days). Longitudinal data were subsequently obtained from 17 of these monkeys at approximately 4-to 8-week intervals until about 300 days of age. Four of the animals in the longitudinal group were normal monkeys reared with unrestricted binocular vision. The other 13 monkeys in the longitudinal group had undergone either monocular laser procedures or unilateral form deprivation of the contralateral eye (Huang et al. *IOVS* 2007, ARVO E-Abstract 1033).²⁰ For these animals, only data for the non-treated eyes are presented.

Ocular Biometry

The basic details of our biometric measurements have been described elsewhere.³⁴ Briefly, to obtain the ocular measurements, each animal was anesthetized with an intramuscular injection of ketamine hydrochloride (15–20 mg/kg) and acepromazine maleate (0.15–0.2 mg/kg). The cornea was anesthetized with 1–2 drops of 0.5% tetracaine hydrochloride. Cycloplegia was achieved by topically instilling 2–3 drops of 1% tropicamide 20–30 minutes before performing any measurement that would potentially be affected by the level of accommodation. During the measurements, the eyelids were gently held apart using a custom made speculum and the corneal tear film was maintained by frequent irrigation using a saline solution.

Central and peripheral refractive errors were measured by streak retinoscopy using hand-held trial lenses. Measurements were obtained at a 50 cm working distance by two well-practiced investigators and the refractions of the most plus and the most minus meridians were recorded in minus cylinder form. All of the refractions for individual eyes represent the arithmetic mean of the results from the two investigators obtained using the matrix approach described by Harris.³⁵ Central refraction was determined along the pupillary axis (i.e., the first Pukinje image produced by the retinoscope beam was observed in the center of the subject's entrance pupil). An arc perimeter with a 45 cm radius that was marked in 15° intervals was used to

facilitate alignment for peripheral refractions. The arc was positioned so that the subject's eye was at the center of the arc; the zero position on the arc was aligned on the pupillary axis using the first Purkinje image as a reference. For measurements along the horizontal meridian, the monkeys were held upright so that the eye's horizontal meridian corresponded to the plane of the arc. Following measurements of the central refraction, retinoscopy was performed at 15° intervals in the nasal and temporal visual fields out to a maximum eccentricity of 45°. The sequence of peripheral refractions was random and following each peripheral measurement, the alignment of the arc was verified by checking whether the first Purkinje image that was formed by the retinoscope positioned at the zero eccentricity was centered in the entrance pupil. For some animals, measurements were also made along the vertical meridian. In these instances, the monkeys were positioned on their sides so that the vertical meridian of the eye to be measured was aligned with the plane of the arc and the pupillary axis was aligned with the zero degree reference on the arc. Measurements were made randomly at 15° intervals in the superior and inferior visual fields. Throughout the paper, eccentricities are specified with respect to the visual field (e.g., temporal field measurements correspond to refractive errors for the nasal retina).

Peripheral retinoscopy is often complicated by the phenomenon of “scissoring” or the so called “double sliding-door effect”.¹ As suggested by Rempt *et al.*¹ the values of refraction were determined when the closing line of both doors was just going through the center of the pupil. There was good agreement between the retinoscopy results for the two examiners, although one observer had a small, but consistent, relative hyperopic bias that was constant throughout the field. For example, for the first measurements along the horizontal meridian, the average differences in spherical-equivalent refractive error between the two retinoscopists (observer 1 – observer 2) were $+0.07 \pm 0.36$ D at the pupillary axis $+0.12 \pm 0.46$ D, $+0.13 \pm 0.75$ D and $+0.12 \pm 0.75$ D at the 15°, 30°, and 45° temporal field eccentricities and $+0.16 \pm 0.56$ D, $+0.24 \pm 0.62$ D, and $+0.02 \pm 1.02$ D at the 15°, 30°, and 45° nasal field eccentricities, respectively. More importantly, the mean peripheral refractions were very repeatable between sessions. For example, Bland-Altman³⁶ plots constructed from the data obtained during the final two measurement sessions for animals in the longitudinal groups (about 266 and 308 days of age; i.e., a period when age-dependent changes would have been minimal) showed that the average limits of agreement (i.e., 1.96 times the standard deviation of the between session differences) were 1.06, 1.03 and 1.21 D for the 15°, 30°, and 45° eccentricities, respectively, and that there were no systematic differences in the repeatability between the nasal and temporal field measures.

Ocular axial dimensions were measured by A-scan ultrasonography implemented with either a 7 (Image 2000; Mentor, Norwell, MA) or 12 MHz transducer (OTI Scan 1000; OTI Ophthalmic Technologies, Inc, Ontario, Canada). The A-scan probe was positioned on the approximate pupillary axis and aligned to maximize the echoes from the cornea, lens, and retina. Intraocular distances were calculated from the average of 10 separate measurements using velocities of 1532, 1641, and 1532 m/sec for the aqueous, lens, and vitreous, respectively. Corneal curvature was measured with a hand-held keratometer (Alcon Auto-keratometer; Alcon Systems Inc, St Louis, MO) and/or a videotopographer (EyeSys 2000; EyeSys technologies Inc, Houston, TX). Both instruments provided repeatable and comparable measures of central corneal curvature in infant monkeys.³⁷

Statistical Analysis

Mixed-design, repeated-measures ANOVAs with Geisser-Greenhouse adjustments (SuperANOVA; Abacus Concepts, Inc, Berkeley, CA) were used to determine if there were differences in the patterns of peripheral refractive errors between eyes with different central refractive errors. One-way or two-way repeated measures ANOVAs with Geisser-Greenhouse

adjustments were used to determine if there were differences in refractive error as a function of eccentricity, differences in the patterns of peripheral refraction between right and left eyes, or changes in the pattern of peripheral refraction with time. Multiple comparisons tests with Geisser-Greenhouse adjustments were subsequently used to compare refractive errors between specific eccentricities and to compare the symmetry of refractive errors along the horizontal and vertical meridians. Linear regression and Pearson correlations were used to examine the relationships between relative peripheral refractive errors and individual optical components and between relative peripheral refractive errors and central refractive errors.

RESULTS

Infant monkeys: Peripheral refraction in the horizontal meridian

As we have previously reported,³⁷ the central refractive errors in the two eyes of our normal 3-week-old monkeys were very similar (right eye: $+3.83 \pm 1.34$ D vs. left eye: $+3.86 \pm 1.35$ D). The average absolute amount of anisometropia for the central retina was 0.24 ± 0.19 D and ranged from $+0.44$ to -0.75 D (right eye – left eye refractive correction). The refractive errors in the two eyes of a given monkey were also well matched across the horizontal meridian and there were no apparent systematic differences between the pattern of peripheral refractive errors in the two eyes ($F = 0.16$, $P = 0.69$; right eye – left eye corrections = -0.09 , -0.03 , $+0.12$ D for the temporal 15° , 30° , and 45° eccentricities, respectively, and $+0.09$, -0.05 , -0.03 D for the nasal 15° , 30° , and 45° eccentricities, respectively). Therefore, in the following cross sectional analyses, only right eye data are shown.

Figure 1A shows the spherical-equivalent refractive corrections plotted as a function of eccentricity along the horizontal meridian for the right eyes of the 58 infants at 24.2 ± 3.7 days of age. Although there was a wide range of central refractive errors ($+0.25$ to $+6.81$ D), all of the infants were hyperopic and the average central refractive error for the group was $+3.83 \pm 1.34$ D (open circle at 0°). The range of peripheral refractive errors was similar to that for the central retina. Moreover, there was relatively little change in refraction across the temporal field; the average refractions were $+3.98 \pm 1.40$ D, $+3.86 \pm 1.45$ D, and $+4.02 \pm 1.37$ D at the 15° , 30° , and 45° temporal eccentricities, respectively ($F = 2.20$, $P = 0.14$). However, a one-way, repeated measures ANOVA revealed that the refractive errors varied as function of eccentricity ($F = 43.34$, $P = 0.001$). Specifically, the refractive states in the nasal field were less hyperopic than the refractive states for either the central retina ($F = 70.65$, $P = 0.0001$) or the temporal field ($F = 195.60$, $P = 0.0001$). The average ametropias in the nasal field were $+3.29 \pm 1.30$ D, $+2.77 \pm 1.23$ D, and $+3.41 \pm 1.25$ D at the 15° , 30° , and 45° eccentricities, respectively.

To better visualize the pattern of peripheral refractions across the horizontal meridian, the peripheral refractive errors for the right eyes of each monkey were normalized to the central refractive error and plotted as a function of eccentricity in Figure 1B. At all temporal field eccentricities the median relative refractive errors were near zero with approximately equal numbers of monkeys exhibiting relative hyperopic and relative myopic refractive errors (55 vs. 41%; 55 vs. 41% and 55 vs. 31% at the 15° , 30° , and 45° temporal field eccentricities, respectively. Note: at each eccentricity a small percentage of animals showed no relative peripheral refractive errors.). In contrast, throughout the nasal field the median refractive errors were consistently less hyperopic / more myopic than the central refractive errors. At the 15° , 30° , and 45° nasal field eccentricities, 93%, 95% and 59% of the infants, respectively, exhibited less hyperopia than was observed in the central retina.

In humans, the pattern of peripheral refractive error varies with the central refractive error.^{6, 8, 11, 15, 38} To examine the relationship between peripheral and central refractive states in infant monkeys, we divided the 58 monkeys into three subgroups based on the degree of central

hyperopia. Specifically, the range of central refractive errors was subdivided into thirds and the data for animals that fell within each of these three equal-dioptic intervals were pooled. Based on this criterion, the average central refractive errors for the animals in the low, moderate and high hyperopic subgroups were $+1.75 \pm 0.66$ D (range = $+0.25$ to $+2.43$ D; $n = 8$), $+3.64 \pm 0.65$ D (range = $+2.44$ to $+4.61$ D; $n = 37$), and $+5.67 \pm 0.57$ D (range = $+4.62$ to $+6.81$ D; $n = 13$), respectively. Figure 2A shows the average refractive errors for these three subgroups plotted as a function of eccentricity; Figure 2B shows the relative peripheral refractive errors for these subgroups normalized to their respective average central refractive errors. A mixed-design, repeated-measures ANOVA revealed that peripheral refraction varied with eccentricity ($F = 41.79$, $P = 0.0001$) and that there were significant differences in the pattern of relative peripheral refractions between subgroups ($F = 5.82$, $P = 0.02$) with significant subgroup-eccentricity interactions ($F = 5.03$, $P = 0.0001$). Specifically, all three subgroups of monkeys showed nasal-temporal asymmetries in peripheral refractive errors (low, $F = 12.82$, $P = 0.02$; moderate, $F = 113.88$, $P = 0.0001$; high, $F = 109.59$, $P = 0.0001$). There were no between-group differences in relative refractions for the temporal field (high vs. low, $F = 0.52$, $P = 0.48$; high vs. moderate, $F = 0.81$, $P = 0.37$; moderate vs. low, $F = 0.007$, $P = 0.94$). However, because there were significant subgroup differences in the nasal field (high vs. low, $F = 10.96$, $P = 0.002$; high vs. moderate, $F = 11.65$, $P = 0.001$; moderate vs. low, $F = 1.20$, $P = 0.28$), the degree of nasal-temporal asymmetries also increased with the degree of central hyperopia. In particular, the relative refractive state in the nasal field was significantly correlated with the eye's vitreous chamber depth at all eccentricities ($r^2 = 0.15$ to 0.22 , $P < 0.003$) and with the central refractive error at the 30° ($r^2 = 0.14$, $P = 0.003$) and 45° eccentricities ($r^2 = 0.23$, $P < 0.0001$), specifically, the shorter and more hyperopic the eye, the higher the degree of relative peripheral myopia in the nasal field. On the other hand, the degree of relative myopia in the nasal field was not correlated with either the central corneal power ($P = 0.14$ to 0.84) or corneal asphericity, as represented by Q values ($P = 0.052$ to 0.26).

The amount of radial astigmatism, particularly against-the-rule astigmatism, increased systematically with horizontal eccentricity. Figure 3A illustrates the average astigmatism, represented by the J_0 and J_{45} vector components ($J_0 = -C \cos(2\theta)/2$; $J_{45} = -C \sin(2\theta)/2$, where C = the power of the minus cylinder correcting lens and θ = the axis of the minus cylinder correcting lens),³⁹ plotted as a function of eccentricity for the right eyes of all 58 infant monkeys. As we have previously reported,³⁷ normal infant monkeys have very little astigmatism along the pupillary axis, but the magnitude of the J_0 component increased in a negative direction (i.e., more against-the-rule astigmatism) to slightly more than one diopter at the 45° eccentricities. The increases in astigmatism were very similar in the nasal and temporal fields. A mixed-design, repeated-measures ANOVA confirmed that the degree of astigmatism increased significantly with eccentricity ($F = 180.65$, $P = 0.0001$) and that there were significant differences in the levels of astigmatism between the different refractive subgroups ($F = 3.24$, $P = 0.05$) with no significant subgroup-eccentricity interactions ($F = 0.83$, $P = 0.62$). In particular, the monkeys in the low hyperopic subgroup showed slightly lower amounts of radial astigmatism (high vs. low, $F = 6.48$, $P = 0.01$; high vs. moderate, $F = 1.82$, $P = 0.18$; Moderate vs. low, $F = 3.30$, $P = 0.07$). These lower amounts of radial astigmatism can not be explained by differences in central corneal power, since the central corneal powers were similar in the three subgroups (average = $+60.17 \pm 1.96$ D, $+59.85 \pm 2.08$ D, and $+60.60 \pm 1.38$ D for the high, moderate, and low hyperopic subgroups, respectively), but may reflect the fact that the monkeys in the low hyperopic subgroup had more oblate shaped corneas (i.e., less negative corneal Q values). The average Q values were 0.00 ± 0.37 , -0.10 ± 0.25 , and -0.20 ± 0.23 for the low, moderate, and high hyperopic subgroups, respectively. However, these differences in Q values were not statistically significant due to large individual variations in each subgroup.

The influence of radial astigmatism on peripheral refractive errors is illustrated in Figure 3B. The average positions of the sagittal and tangential image planes are plotted as a function of eccentricity for the low, moderate, and high hyperopic subgroups. In the temporal field, all of the subgroups demonstrated mixed astigmatism relative to the pupillary axis, i.e., on average, the tangential meridian was relatively more myopic and the sagittal meridian was relatively more hyperopic than the central ametropia. In the nasal field, relative to the central ametropia, the high hyperopic subgroup showed compound myopic astigmatism at all eccentricities and the moderate hyperopic subgroup exhibited compound myopic astigmatism at the 15° and 30° eccentricities. In contrast, the low hyperopic subgroup demonstrated essentially simple myopic astigmatism at the 15° and 30° eccentricities and mixed astigmatism at the 45° nasal field eccentricity.

Infant monkeys: Peripheral refraction in the vertical meridian

Peripheral refractions along the vertical meridian were first measured at 61 ± 10 days of age; hence data are only available for the 17 monkeys that were followed longitudinally. As shown in Figure 4A, the average spherical-equivalent refractive errors were relatively constant across the superior field; however, the average refractive errors at the 15° and 30° eccentricities in the inferior field were significantly more myopic / less hyperopic than the average central refractive error ($F = 13.49$, $P = 0.004$). The pattern of peripheral refractive errors in the inferior field was very consistent from animal to animal (Figure 4B). All 17 animals exhibited relative myopia at the inferior 15° and/or 30° eccentricities. In contrast, in the superior field, relative myopia and relative hyperopia were observed in approximately equal numbers of animals and the superior field refractions were not significantly different from the average central refraction ($F = 0.12$, $P = 0.57$).

As in the horizontal meridian, the degree of radial astigmatism increased symmetrically in the inferior and superior fields. The degree of with-the-rule astigmatism in the inferior and superior fields was similar at each eccentricity (inferior field vs. superior field; 15° eccentricities: 0.40 ± 0.29 D vs. 0.24 ± 0.54 D; 30° eccentricities: 1.27 ± 0.84 D vs. 1.07 ± 0.76 D; 45° eccentricities: 2.48 ± 0.75 D vs. 2.01 ± 1.07 D) and comparable to the amounts of against-the-rule astigmatism observed along the horizontal meridian (see Figure 8 below). At all vertical eccentricities, the average sagittal and tangential image shells were more hyperopic and more myopic, respectively, than the central refractive error, i.e., on average the infants showed mixed astigmatism at all eccentricities along the vertical meridian.

Longitudinal changes in peripheral refraction

Although monocular experimental manipulations can result in interocular effects in infant monkeys,⁴⁰ as illustrated in Figure 5, emmetropization proceeded in an apparently normal manner in the non-treated eyes of the 13 infants in the longitudinal group that had experimental manipulations performed on their fellow eyes. The central refractive errors for the non-treated eyes were within the range of refractive errors for normal monkeys throughout most of the observation period and the distributions of refractive errors at the end of the period of rapid emmetropization (about 160 days of age) were comparable for the normal and non-treated fellow eyes. Hence, for this study, we assumed that the non-treated eyes were normal.

To examine how the peripheral refractions changed during emmetropization, the 17 monkeys that were followed longitudinally were segregated into subgroups based on their central refractive errors at 3 weeks of age using the same criterion described above. Figure 6 shows the average spherical-equivalent refractive errors (top) and the relative peripheral refractive errors (bottom) along the horizontal meridian at 3 weeks of age (open circles) and at 308 ± 13 days of age (filled circles) (i.e., after the rapid period of emmetropization). The monkeys with

low ($n = 4$), moderate ($n = 10$), and high amounts of central hyperopia ($n = 3$) are shown in the left, middle, and right columns, respectively.

The pattern of peripheral refractive errors in the horizontal meridian obtained from the longitudinal subgroups at 3 weeks of age was comparable to that shown above for the larger cross-sectional group of infants. In particular, there were obvious nasal-temporal asymmetries ($F = 80.61$, $P = 0.0001$). Whereas, the spherical-equivalent refractive errors were relatively constant (moderate and high hyperopes) or slightly more hyperopic (low hyperopes) across the temporal field, the peripheral refractions were relatively more myopic in the nasal field, especially at the 15° and 30° eccentricities, and the degree of relative myopia in the nasal field increased with the degree of central hyperopia (nasal field 15° , $r^2 = 0.23$, $P = 0.06$; nasal field 30° , $r^2 = 0.56$, $P < 0.001$).

During emmetropization there was a decrease in the average degree of central hyperopia in all three subgroups and, as expected, the amount of change was directly related to the initial degree of central hyperopia ($r^2 = 0.92$, $P < 0.0001$). Consequently, after the rapid period of emmetropization, the central refractive errors were very similar in all three subgroups (high hyperopes = $+1.79 \pm 0.13$ D; moderate = $+2.18 \pm 0.42$ D; low = $+1.94 \pm 0.31$ D). The pattern and magnitude of peripheral refractive errors also became more similar between the three subgroups over time. A two-way, repeated-measures ANOVA showed that the pattern of relative peripheral refractive errors changed significantly with time ($F = 5.80$, $P = 0.003$). Specifically, by 308 days of age, the pattern of peripheral refractions in the nasal and temporal fields was more symmetrical with all subgroups exhibiting similar amounts of relative myopia in both the nasal and temporal fields (see Table 1) (nasal vs. temporal: $F = 3.11$, $P = 0.10$). The manner in which this pattern of peripheral refraction was achieved varied somewhat between the three subgroups. For example, for the monkeys in the high central hyperopia subgroup, there was a decrease in relative myopia in the nasal field, whereas, in the moderate and low hyperopic subgroups, the relative peripheral refractions in the nasal field were comparatively stable and the final pattern of peripheral refractive errors came about primarily by an increase in the relative myopia in the temporal field.

Because there were no significant differences in the pattern of peripheral refractions in the vertical meridian between the different central refractive error subgroups at either 61 or 260 days of age (mixed-design, repeated-measures ANOVAs: at 61 days, $F = 0.002$, $P = 0.99$; at 260 days $F = 0.08$, $P = 0.93$), data for all 17 of the monkeys that were followed longitudinally were combined. Figure 7 shows the average (top) and relative peripheral refractions (bottom) in the vertical meridian at 61 (open circles) and 260 days of age (filled circles). The pattern of refraction was asymmetric at 61 days of age. There was a statistically significant difference between the relative refractive errors in the inferior and superior fields ($F = 12.03$, $P = 0.005$), with the inferior field being more myopic. Between 61 and 260 days, the average central hyperopia changed very little ($+2.42 \pm 0.92$ D vs. $+2.40 \pm 0.54$ D). There were also no changes in the relative peripheral refractive errors in the inferior field; at both ages, the monkeys showed essentially the same amounts of relative myopia at the 15° and 30° eccentricities (inferior field 15° : -0.44 ± 0.41 D vs. -0.37 ± 0.33 D at 61 and 260 days of age, respectively; inferior field 30° : -0.60 ± 0.79 D vs. -0.67 ± 0.53 D at 61 and 260 days of age, respectively) and essentially no relative refractive myopia at the 45° eccentricity ($+0.20 \pm 1.30$ D at 61 days of age and $+0.01 \pm 0.78$ D at 260 days of age). In the superior field, however, the average refraction at the 30° eccentricity showed a small amount of relative myopia at 260 days of age (-0.42 ± 0.42 D). Consequently, at 260 days there were no significant differences in the pattern of peripheral refraction between the inferior and superior fields ($F = 3.65$, $P = 0.08$).

Figure 8 shows the changes in radial astigmatism (i.e., $J_0 \times 2$) that took place in the horizontal meridian between 24 and 308 days of age and in the vertical meridian between 61 and 260 days

of age. There was a modest, but significant, decrease in the amount of radial astigmatism in both the horizontal ($F = 29.51$, $P = 0.001$) and vertical meridians ($F = 10.82$, $P = 0.005$). These decreases in radial astigmatism were symmetrical in a given meridian and similar in magnitude in the vertical and horizontal meridian. For example, at the 45° eccentricities the average decreases in the amount of astigmatism were -0.59 ± 0.69 D, -0.73 ± 0.75 D, -0.69 ± 0.80 D and -0.30 ± 1.15 D for the nasal, temporal, inferior, and superior fields, respectively. However, the magnitudes of radial astigmatism were still large in comparison to the relative spherical-equivalent refractive errors in the periphery. As a consequence, at the end of the observation period all of the subjects showed mixed astigmatism at all eccentricities in both the vertical and horizontal meridians (i.e., relative myopia and hyperopia in the tangential and sagittal image planes, respectively).

DISCUSSION

The major findings in infant monkeys were that 1) the degree of astigmatism increased systematically and symmetrically with eccentricity along the horizontal and vertical meridians, 2) the average spherical-equivalent refractive errors in the temporal and superior fields were similar to the central ametropia, however, the peripheral refractions in the nasal and inferior fields were less hyperopic / more myopic than the central ametropia, and 3) the relative myopia in the nasal field increased with the degree of central hyperopia. During early development, we found that 1) there was a decrease in radial astigmatism in all semi meridians, 2) emmetropization, as assessed by the spherical-equivalent refractive correction, occurred in both the peripheral and central fields, and 3) the peripheral refractions along the horizontal and vertical meridians became more symmetrical.

All of our retinoscopy measures are potentially influenced by the artifact of retinoscopy, which is believed to arise from the fact that the retinoscopy reflex is produced at the vitreo-retinal interface rather than at the photoreceptor level.⁴¹ We have previously reported that in young monkeys there are systematic differences between the refractive errors measured behaviorally and those obtained by retinoscopy or with an autorefractor.⁴² Specifically, on average, autorefractor and retinoscopy measures are between +1.25 and +1.50 D more hyperopic, than subjective measures in young monkeys.

However, it is unlikely that this discrepancy influenced our main conclusions. First, at a given retinal location the artifact of retinoscopy would not affect the measured degree of astigmatism because both meridians would be referenced to the same location and the dioptric differences in refractive errors would not be affected by the position of the reference plane.

With respect to the pattern of peripheral refractions (i.e., the spherical equivalent errors), the artifact of retinoscopy could theoretically change the pattern of peripheral refraction if there were significant differences in vitreous chamber depth between the central and peripheral retina (as in prolate or oblate shaped eyes) or if retinal thickness varied substantially with eccentricity. For example, assume that the foveal retinal thickness is 288 microns (This represents the average of the maximum thicknesses obtained by OCT just nasal and temporal to the center of the fovea in 3 adolescent monkeys. Wheat and Harwerth, personal communication) and that the outer limiting membrane is located at a depth 192 microns (70% of the total thickness; the presumed location of the photoreceptor apertures). Based on a schematic eye model for young monkeys,⁴³ the theoretical artifact of retinoscopy at the fovea would be +1.15 D, which corresponds closely to the differences between retinoscopic and subjective measures of refractive errors in young monkeys.⁴² First, consider how changes in the shape of the posterior globe would influence the magnitude of this artifact. Assume that the eye is oblate in shape (and that there were no eccentricity-dependent changes in retinal thickness) and that there is a 0.5 mm difference in the vitreous chamber depth between the fovea and an eccentricity of 45°

degree (This is 2 times larger than the largest axial length change that we have observed in MRI images over the central 45 degrees in 300-day-old normal monkeys (Huang et al. *IOVS* 2008; ARVO E-Abstract 3588). The theoretical artifact of retinoscopy at the 45 degree eccentricity would be +1.08 D, i.e., 0.07 D different from that at the fovea. Thus, it is unlikely that variations in the artifact of retinoscopy due to effective changes in vitreous chamber depth influenced our results.

However, it is known that retinal thickness decreases with eccentricity,^{44,45} which could potentially have a larger effect on the artifact of retinoscopy. Peripheral OCT scans obtained on 3 adolescent monkeys showed that at temporal and nasal eccentricities of about 35 degree the retinas were on average 168 and 187 microns thick, respectively. Thus, in comparison to the fovea the artifact of retinoscopy would decrease to +0.79 and +0.71 D in the temporal and nasal retinas, respectively. In other words, the peripheral retina would theoretically appear to be about 0.4 D less hyperopic or more myopic than the central retina due to changes in retinal thickness. In this respect, it is possible that variations in retinal thickness contributed, at least in part, to the relative peripheral myopia observed at some eccentricities in our monkeys. However, it is unlikely that alterations in retinal thickness can explain the patterns of peripheral refractive errors that we observed. In particular, the asymmetries observed in the horizontal and vertical meridians in young animals and the fact that in a given semi-meridian the degree of relative hyperopia first increases at small eccentricities and then decreases at larger eccentricities (at 45 deg). Furthermore, the variations in the pattern of peripheral refractions with central refractive error and the changes in these patterns with age are also unlikely to be influenced by the variations in retinal thickness and the artifact of retinoscopy

Little is known about peripheral refractions in human infants. As a consequence, comparisons between our results from infant monkeys and the data available from relatively older humans are potentially influenced by developmental factors. With respect to peripheral astigmatism, both infant monkeys and humans exhibit systematic increases with eccentricity. There are, however, some apparent quantitative differences. Specifically, the range and average degree of peripheral astigmatism in our infant monkeys were slightly lower than in children or adult humans. For example, at a horizontal eccentricity of 30° the against-the-rule astigmatic errors in the horizontal meridian varied between 0.25 and 2.75 D in our infant monkeys versus a range of 1 to 7 D in emmetropic adult humans.⁷ The average against-the-rule astigmatic errors at a horizontal eccentricity of 30° in our 24-day-old monkeys was 1.10 ± 0.44 D, whereas, for emmetropic humans the average against-the-rule error at a 30° eccentricity is 1.84 ± 0.46 D.^{3,4,7,46,47} Since the amount of astigmatism decreased with age in our monkeys, these differences between humans and monkeys are likely to reflect interspecies differences in the shape of the peripheral cornea and/or the crystalline lens rather than age differences.

There were also small differences between humans and monkeys in the nasal-temporal symmetry of the astigmatic errors. In infant monkeys, the measured astigmatic errors increased symmetrically in the nasal and temporal fields. In contrast, in humans it has commonly been reported that the degree of against-the-rule astigmatism increases faster with eccentricity in the nasal field than in the temporal field.^{3,48} It is likely that this apparent discrepancy reflects differences in the reference axes. In humans, eccentric measurements are almost always made with respect to the visual axis, whereas, in our study the pupillary axis was used as the reference axis. Because angle alpha is typically positive in humans,⁴⁹ the corneal apex and the optical axis are located temporally with respect to the visual axis and, thus in humans, eccentricities are usually not referenced symmetrically with respect to the eye's presumed optical axis.^{3,48} Consequently, it is likely that the resulting rotation and translation of the cornea and lens relative to the visual axis contributes to the observed nasal-temporal asymmetries in humans,^{48,50} In contrast, the greater symmetry observed in monkeys probably reflects the fact that the pupillary axis is more closely aligned to the presumed optical axis.

Our Infant monkeys, like many humans, exhibited asymmetries in their spherical-equivalent refractive errors along the horizontal meridian and the patterns in the two eyes were always very similar. In particular, like many hyperopic children and adult humans,^{6,8,11,15} our infant monkeys, which invariably had hyperopic central ametropias, exhibited relatively lower amounts of hyperopia (i.e., relative myopia) at the 15° and 30° eccentricities in the nasal field than at comparable eccentricities in the temporal field. Because the radial astigmatism in our infant monkeys was symmetrical along the horizontal and vertical meridians, it is likely that the nasal-temporal and superior-inferior asymmetries in spherical refractive error reflect asymmetries in the shape of the posterior globe.¹⁴ Specifically, these data suggest that the vitreous chamber of the infant monkey eye is effectively deeper in the temporal and superior hemi-retinal areas and that this shape asymmetry in the horizontal meridian increases with the degree of central hyperopia.

The fact that the degree of relative peripheral myopia in the nasal field increased with increasing amounts of central hyperopia in infant monkeys is also somewhat analogous to the relationship between the pattern of peripheral refractions and central refractive errors that have been reported in humans. Specifically, studies in humans indicate that whereas myopic subjects usually exhibit relative hyperopia in the periphery, emmetropes typically exhibit a small degree of relative peripheral myopia and hyperopes usually show the highest average degree of relative peripheral myopia.^{6,8,11,15,38} In other words, as in our infant monkeys, peripheral refractions in humans become relatively more myopic as the central refraction becomes more hyperopic.

It has been argued that the associations between peripheral and central refractive errors that have been observed in children and adults come about because peripheral refractive errors influence central refractive development.^{18,19,21} In particular, it has been hypothesized that relative peripheral myopia would promote central hyperopia in children and adults. Although there are parallels between the pattern of peripheral refractions in hyperopic infant monkeys and older humans, our monkey data do not necessarily support this idea. Specifically, it seems unlikely that the association between peripheral myopia and the degree of central hyperopia that we found in infants is causal in nature and came about as a consequence of vision-dependent growth. Given that we observed this relationship at a very young age (2–3 weeks of age), it seems more likely, at least in hyperopic infant eyes, that the variations in the pattern of peripheral refractive errors reflect programmatic differences in posterior globe shape that are associated with absolute differences in axial length, in essence, these shape differences are probably a consequence of a pre-programmed genetic growth process. This idea is reinforced by the fact that with time the highly hyperopic eyes in the longitudinal group that showed relative peripheral myopia underwent emmetropization. In this respect, there is a key difference between the relative peripheral myopia observed in hyperopic humans and infant monkey eyes. Whereas all of our monkeys demonstrated emmetropization early in life and a concomitant reduction in relative peripheral myopia, hyperopic humans may have maintained their central and peripheral errors throughout infancy. Perhaps the pattern of peripheral refraction in hyperopic children and adult humans was present shortly after birth and persisted because the degree of central hyperopia was outside the operating range of the emmetropization mechanism³⁴ and/or the relative peripheral myopia was larger than some critical amount and thus dominated ocular development. It is interesting that some presumably normal monkeys (e.g., the solid symbols in Figure 5) also maintain relatively high hyperopic errors throughout infancy. Unfortunately, peripheral refractions have not been assessed in these animals.

Along the vertical meridian, our infant monkeys exhibited relative myopia in the inferior field. This asymmetry appears to be analogous to the lower-field myopia that has been observed in many different animal species^{31,32,51,52} (See Smith⁵³ for a review) and that has been reported in humans in some,⁸ but not all studies.⁴⁷ It has been argued that lower-field myopia represents a functional adaptation that promotes panoramic vision. Specifically, lower field

myopia in emmetropic animals can help keep objects on the ground in focus while the animal maintains an unaccommodated state and fixation at the horizon.³¹

Since experimentally imposed variations in visual experience across the visual field can produce compensating local changes in eye shape in some species, it has been hypothesized that lower field myopia may be a consequence of normal emmetropization.³³ However, the fact that we observed these vertical asymmetries in our earliest measurements in infant monkeys suggests that the relative myopia observed in the inferior field of our infant monkeys reflects a congenital asymmetry, not an emmetropizing response associated with potentially restricted viewing distances in the inferior field. However, it should be kept in mind that our first measurements in the vertical meridian were obtained when the animals were about 60 days of age and it is possible lower field myopia could have developed between birth and 60 days of age.

In addition to the expected changes in central refraction, the ocular changes associated with emmetropization reduced the absolute peripheral refractive errors and altered the pattern of peripheral refractions. It was particularly impressive that by about 300 days of age all of the monkeys, regardless of their initial degree of central hyperopia, demonstrated either no relative spherical refractive errors or small degrees of relative myopia in the periphery. As a consequence, relative to the central retina, all of the monkeys exhibited either mixed astigmatism or simple myopic astigmatism at each peripheral eccentricity. In addition, there were no significant nasal-temporal or superior-inferior asymmetries in peripheral refraction. Thus, after achieving the central target refractive state for emmetropization, these young monkeys showed peripheral refraction patterns that were very comparable to those for the average emmetropic adult human.^{2,8,11} In this respect, it appears that the target refractive state for emmetropization in the periphery of the primate eye is a small degree of relative myopia.

Because all of the 308-day-old animals had similar central refractive errors, it may not seem surprising that all of these animals showed similar patterns of peripheral refractions. However it is important to note that while all of our infants demonstrated substantial absolute increases in axial length, the changes in peripheral refraction varied substantially between monkeys. For instance, in the low hyperopic subgroup, there were reductions in relative peripheral hyperopia, whereas the high hyperopic subgroup showed reductions in relative peripheral myopia. Given that all of the infants exhibited increases in axial length, the different changes in peripheral refraction found in different individuals suggest that during emmetropization the shape of the posterior globe is actively regulated and altered to optimize image clarity across the retina. This idea is plausible because it is well documented that variations in focus across the visual field can produce changes in the shape of the posterior globe in chickens²⁸ and tree shrews.³⁰ However, to date, the presence of local retinal mechanisms, which are believed to be responsible for these vision-induced shape changes, have not been conclusively demonstrated in primates.

The very consistent pattern of peripheral refractions found in our monkeys at the end of the early period of emmetropization has implications for the pattern of peripheral refractive errors observed in juvenile and adult myopic humans. Specifically, because the course of emmetropization and the ocular changes that occur during early refractive development are very similar in humans and macaques, our data suggest that at around 3 years of age (i.e., ages equivalent to those of our oldest monkeys),^{43,54} when the variance of central refractive errors in children is very small, the patterns of peripheral refraction will also be very similar with most children exhibiting small amounts of relative peripheral myopia. If this is correct, then the different patterns of peripheral refraction found in myopic versus emmetropic adults must develop after the early rapid period of emmetropization. In this respect, Mutti et al.¹³ have recently found that relative peripheral hyperopia develops in children several years prior to the

onset of central myopia, but well after the early period of emmetropization. It seems plausible that the different patterns of peripheral refractions found in myopic versus hyperopic humans emerge at different ages. Eyes that eventually become myopic may manifest this pattern after the early rapid period of emmetropization, whereas in eyes that maintain or develop high degrees of hyperopia, the pattern may be present very early in life and persist throughout childhood.

During emmetropization there were also concomitant reductions in peripheral astigmatism in both the vertical and horizontal meridians. However, it is likely that these astigmatic changes are passive in nature and reflect, at least partially, the overall reduction in corneal power, which for the central cornea decreased from $+60.49 \pm 2.14$ D at 24 days of age to about $+52.78 \pm 1.84$ D at 308 days of age. Interestingly, the average corneal Q value did not change during this age period (-0.01 ± 0.22 at 24 days of age vs. -0.02 ± 0.19 at 308 days of age).

In near-emmetropic humans, peripheral refractive errors, especially relative hyperopic errors, are a risk factor for the onset and progression of myopia.¹⁶ In animal models, peripheral visual signals can have a significant influence on central refractive development.^{18–21} Thus, it is reasonable to ask whether peripheral refractive errors contribute to emmetropization under normal circumstances. In this respect, since infant monkeys generally exhibit significant amounts of central hyperopia and they do not appear to accommodate consistently to eliminate their central refractive errors,⁵⁵ it is probably important to consider absolute, rather than relative, refractive errors in the periphery. All of our infant monkeys exhibited absolute hyperopic refractions in the periphery that would presumably elicit growth signals that were complimentary to those associated with the central hyperopic errors. Consequently, it is reasonable to suppose that signals from the peripheral retina normally facilitate emmetropization for the central retina in infant monkeys.

Acknowledgements

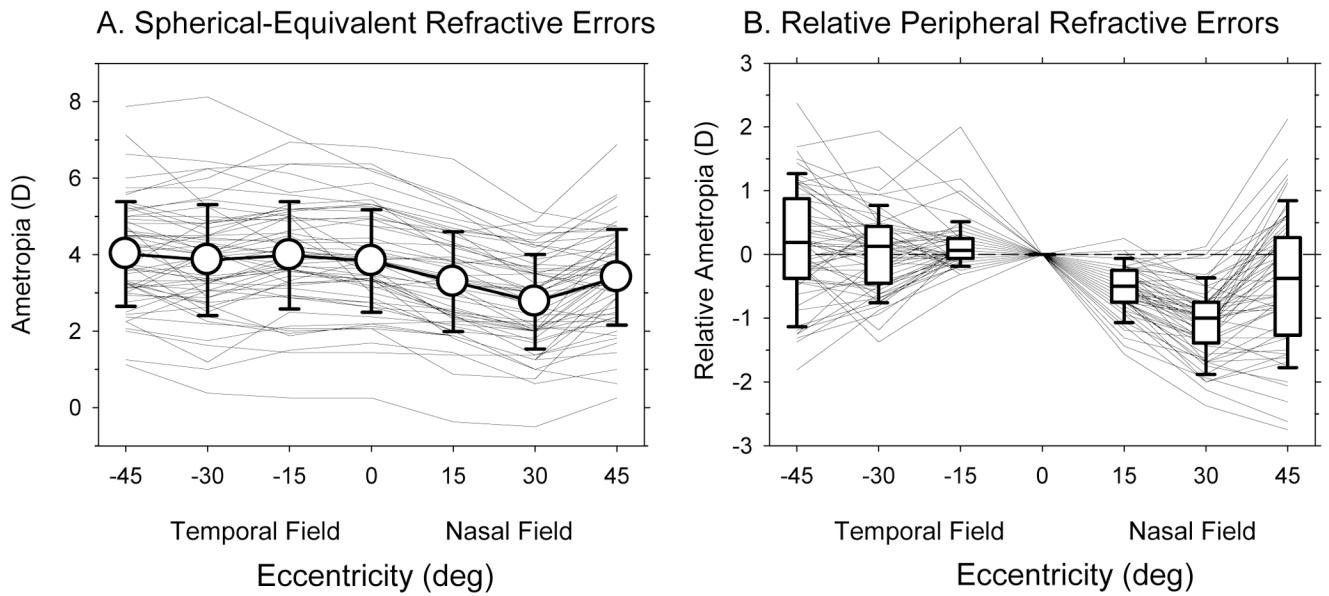
This work was supported by NIH Grants EY-03611, EY-07551 and funds from the Vision CRC and the UH Foundation.

References

1. Rempt F, Hoogerheide J, Hoogenboom WP. Peripheral retinoscopy and the skiagram. *Ophthalmologica* 1971;162:1–10. [PubMed: 5547863]
2. Charman WN, Jennings JA. Longitudinal changes in peripheral refraction with age. *Ophthalmic Physiol Opt* 2006;26:447–455. [PubMed: 16918768]
3. Lotmar W, Lotmar T. Peripheral astigmatism in the human eye: experimental data and theoretical model predictions. *J Opt Soc Am* 1974;64:510–513. [PubMed: 4822573]
4. Ferree CE, Rand G, Hardy C. Refraction for the peripheral field of vision. *Arch Ophthalmol* 1931;5:717–731.
5. Millodot M, Lamont A. Letter: Refraction of the periphery of the eye. *J Opt Soc Am* 1974;64:110–111. [PubMed: 4813433]
6. Millodot M. Effect of ametropia on peripheral refraction. *Am J Optom Physiol Opt* 1981;58:691–695. [PubMed: 7294139]
7. Gustafsson J, Terenius E, Buchheister J, Unsbo P. Peripheral astigmatism in emmetropic eyes. *Ophthalmic Physiol Opt* 2001;21:393–400. [PubMed: 11563427]
8. Seidemann A, Schaeffel F, Guirao A, Lopez-Gil N, Artal P. Peripheral refractive errors in myopic, emmetropic, and hyperopic young subjects. *J Opt Soc Am A Opt Image Sci Vis* 2002;19:2363–2373. [PubMed: 12469730]
9. Ferree CE, G R, C H. Refractive asymmetry in the temporal and nasal halves of the visual field. *Am J Ophthalmol* 1932;15:513–522.

10. Ferree CE, Rand G. Interpretation of refractive conditions in the peripheral field of vision. *Arch Ophthalmol* 1933;9:925–938.
11. Atchison DA, Pritchard N, White SD, Griffiths AM. Influence of age on peripheral refraction. *Vision Res* 2005;45:715–720. [PubMed: 15639498]
12. Mutti DO, Hayes JR, Mitchell GL, et al. Refractive error, axial length, and relative peripheral refractive error before and after the onset of myopia. *Invest Ophthalmol Vis Sci* 2007;48:2510–2519. [PubMed: 17525178]
13. Mutti DO, Zadnik K, Hayes JR, Mitchell GL, Jones LA, Moeschberger ML. Axial length and ocular shape before and after the onset of myopia. *Optom Vis Sci* 2004;12:24.
14. Logan NS, Gilmartin B, Wildsoet CF, Dunne MC. Posterior retinal contour in adult human anisomyopia. *Invest Ophthalmol Vis Sci* 2004;45:2152–2162. [PubMed: 15223789]
15. Mutti DO, Sholtz RI, Friedman NE, Zadnik K. Peripheral refraction and ocular shape in children. *Invest Ophthalmol Vis Sci* 2000;41:1022–1030. [PubMed: 10752937]
16. Hoogerheide J, Rempt F, Hoogenboom WP. Acquired myopia in young pilots. *Ophthalmologica* 1971;163:209–215. [PubMed: 5127164]
17. Schmid G. Retinal steepness vs. myopic shift in children. *Optom Vis Sci* 2004;12:23.
18. Smith EL III, Kee CS, Ramamirtham R, Qiao-Grider Y, Hung LF. Peripheral vision can influence eye growth and refractive development in infant monkeys. *Invest Ophthalmol Vis Sci* 2005;46:3965–3972. [PubMed: 16249469]3rd
19. Stone RA, Flitcroft DI. Ocular shape and myopia. *Ann Acad Med Singapore* 2004;33:7–15. [PubMed: 15008555]
20. Smith EL III, Ramamirtham R, Qiao-Grider Y, et al. Effects of foveal ablation on emmetropization and form-deprivation myopia. *Invest Ophthalmol Vis Sci* 2007;48:3914–3922. [PubMed: 17724167]
21. Wallman J, Winawer J. Homeostasis of eye growth and the question of myopia. *Neuron* 2004;43:447–468. [PubMed: 15312645]
22. Napper GA, Brennan NA, Barrington M, Squires MA, Vessey GA, Vingrys AJ. The effect of an interrupted daily period of normal visual stimulation on form deprivation myopia in chicks. *Vision Res* 1997;37:1557–1564. [PubMed: 9231222]
23. Smith EL III, Hung LF, Kee C-s, Qiao Y. Effects of brief periods of unrestricted vision on the development of form-deprivation myopia in monkeys. *Invest Ophthalmol Vis Sci* 2002;43:291–299. [PubMed: 11818369]
24. Schmid KL, Wildsoet CF. Effects on the compensatory responses to positive and negative lenses of intermittent lens wear and ciliary nerve section in chicks. *Vision Res* 1996;36:1023–1026. [PubMed: 8736261]
25. Napper GA, Brennan NA, Barrington M, Squires MA, Vessey GA, Vingrys AJ. The duration of normal visual exposure necessary to prevent form deprivation myopia in chicks. *Vision Res* 1995;35:1337–1344. [PubMed: 7610595]
26. Kee CS, Hung LF, Qiao-Grider Y, et al. Temporal constraints on experimental emmetropization in infant monkeys. *Invest Ophthalmol Vis Sci* 2007;48:957–962. [PubMed: 17325132]
27. Wallman J, Gottlieb MD, Rajaram V, Fugate-Wentzek LA. Local retinal regions control local eye growth and myopia. *Science* 1987;237:73–77. [PubMed: 3603011]
28. Diether S, Schaeffel F. Local changes in eye growth induced by imposed local refractive error despite active accommodation. *Vision Res* 1997;37:659–668. [PubMed: 9156210]
29. Hodoss W, Kuenzel WJ. Retinal-image degradation produces ocular enlargement in chicks. *Invest Ophthalmol Vis Sci* 1984;25:652–659. [PubMed: 6724835]
30. Norton TT, Siegwart JT. Animal models of emmetropization: matching axial length to the focal plane. *J Am Optom Assoc* 1995;66:405–414. [PubMed: 7560727]
31. Fitzke FW, Hayes BP, Hodoss W, Holden AL, Low JC. Refractive sectors in the visual field of the pigeon eye. *J Physiol* 1985;369:33–44. [PubMed: 4093886]
32. Hodoss W, Erichsen JT. Lower-field myopia in birds: an adaptation that keeps the ground in focus. *Vision Res* 1990;30:653–657. [PubMed: 2378058]
33. Miles FA, Wallman J. Local ocular compensation for imposed local refractive error. *Vision Res* 1990;30:339–349. [PubMed: 2336793]

34. Smith EL III, Hung LF. The role of optical defocus in regulating refractive development in infant monkeys. *Vision Res* 1999;39:1415–1435. [PubMed: 10343811]
35. Harris WF. Algebra of spherocylinders and refractive errors, and their means, variance, and standard deviation. *Am J Optom Physiol Opt* 1988;65:794–802. [PubMed: 3207150]
36. Bland JM, Altman DG. Statistical methods for assessing agreement between two methods of clinical measurement. *Lancet* 1986;1:307–310. [PubMed: 2868172]
37. Kee, C-s; Hung, L-F.; Qiao, Y.; Habib, A.; Smith, EL, III. Prevalence of Astigmatism in Infant Monkeys. *Vision Res* 2002;42:1349–1359. [PubMed: 12044741]
38. Seidemann A, Schaeffel F. Effects of longitudinal chromatic aberration on accommodation and emmetropization. *Vision Res* 2002;42:2409–2417. [PubMed: 12367740]
39. Thibos LN, Wheeler W, Horner D. Power vectors: an application of fourier analysis to the description and statistical analysis of refractive error. *Optom & Vision Sci* 1997;74:367–375.
40. Bradley DV, Fernandes A, Boothe RG. The refractive development of untreated eyes of rhesus monkeys varies according to the treatment received by their fellow eyes. *Vision Res* 1999;39:1749–1757. [PubMed: 10343866]
41. Glickstein M MM. Retinoscopy and eye size. *Science* 1970;168:605–606. [PubMed: 5436596]
42. Ramamirtham R, Kee C-s, Hung L-F, Qiao Y, Harwerth RS, Smith EL III. Comparison of objective and subjective refractions in *Macaca Mulatta*. *Optom Vis Sci* 2001;78:90.
43. Qiao-Grider Y, Hung LF, Kee CS, Ramamirtham R, Smith EL 3rd. Normal ocular development in young rhesus monkeys (*Macaca mulatta*). *Vision Res* 2007;47:1424–1444. [PubMed: 17416396]
44. Jakobiec FA. *Ocular Anatomy, Embryology and Teratology* 1982:7.
45. Salzman M. *The Anatomy and Histology of Human Eyeball in the Normal State; Its development and senescence.* 1912:63.
46. Millodot M, Lamont A. Refraction of the periphery of the eye. *J of the Optical Society of America* 1973;64:110–111.
47. Atchison DA, Pritchard N, Schmid KL. Peripheral refraction along the horizontal and vertical visual fields in myopia. *Vision Res* 2006;46:1450–1458. [PubMed: 16356528]
48. Dunne MC, Misson GP, White EK, Barnes DA. Peripheral astigmatic asymmetry and angle alpha. *Ophthalmic Physiol Opt* 1993;13:303–305. [PubMed: 8265173]
49. Barry JC, Effert R, Kaupp A. Objective measurement of small angles of strabismus in infants and children with photographic reflection pattern evaluation. *Ophthalmology* 1992;99:320–328. [PubMed: 1565443]
50. Barnes DA, Dunne MC, Clement RA. A schematic eye model for the effects of translation and rotation of ocular components on peripheral astigmatism. *Ophthalmic Physiol Opt* 1987;7:153–158. [PubMed: 3658439]
51. Murphy CJ, Howland M, Howland HC. Raptors lack lower-field myopia. *Vision Res* 1995;35:1153–1155. [PubMed: 7610576]
52. Schaeffel F, Hagel G, Eikermann J. Lower-field myopia and astigmatism in amphibians and chickens. *J Opt Soc Am A* 1994;11:487–495.
53. Smith, EL, III. Environmentally induced refractive errors in animals. In: Rosenfield, M.; Gilmartin, B., editors. *Myopia and Nearwork*. Oxford: Butterworth-Heinemann; 1998. p. 57-90.
54. Bradley DV, Fernandes A, Lynn M, Tigges M, Boothe RG. Emmetropization in the rhesus monkey (*Macaca mulatta*): birth to young adulthood. *Invest Ophthalmol Vis Sci* 1999;40:214–229. [PubMed: 9888446]
55. Boothe RG, Dobson V, Teller DY. Postnatal development of vision in human and nonhuman primates. *Annu Rev Neurosci* 1985;8:495–545. [PubMed: 3920945]

**Figure 1.**

A. Spherical-equivalent refractive errors plotted as a function of horizontal eccentricity. Thin solid lines represent the right eyes of individual monkeys. The open circles represent the averages (\pm SD) for all 58 monkeys. B. The peripheral refractions of individual monkeys normalized to their central refractive errors plotted as a function of horizontal eccentricity. Thin solid lines represent individual monkeys. The lines in the box plots represent the medians. The boundaries of the box plots indicate the 25th and the 75th percentiles. The error bars above and below the boxes indicate the 90th and 10th percentiles, respectively.

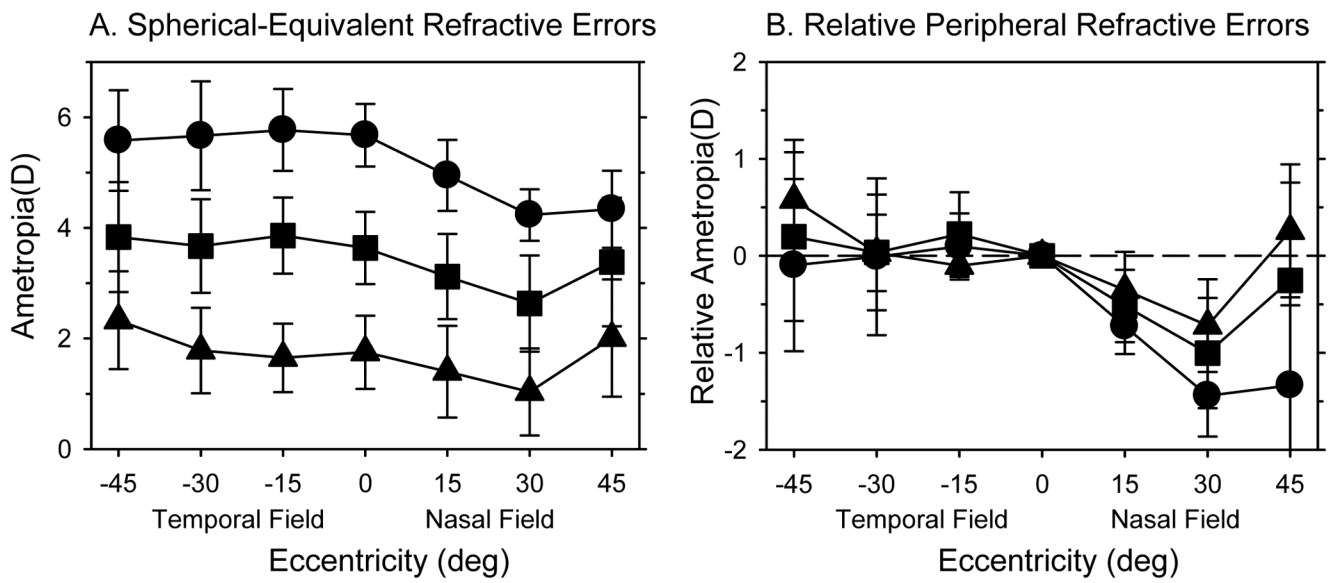


Figure 2. A. Average spherical-equivalent refractive errors (\pm SD) plotted as a function of horizontal eccentricity for the right eyes of the monkeys in the high (filled circles), moderate (filled squares) and low hyperopic subgroups (filled triangles). B. Average peripheral refractions measured relative to the average central refractions plotted as a function of horizontal eccentricity for the same subgroups.

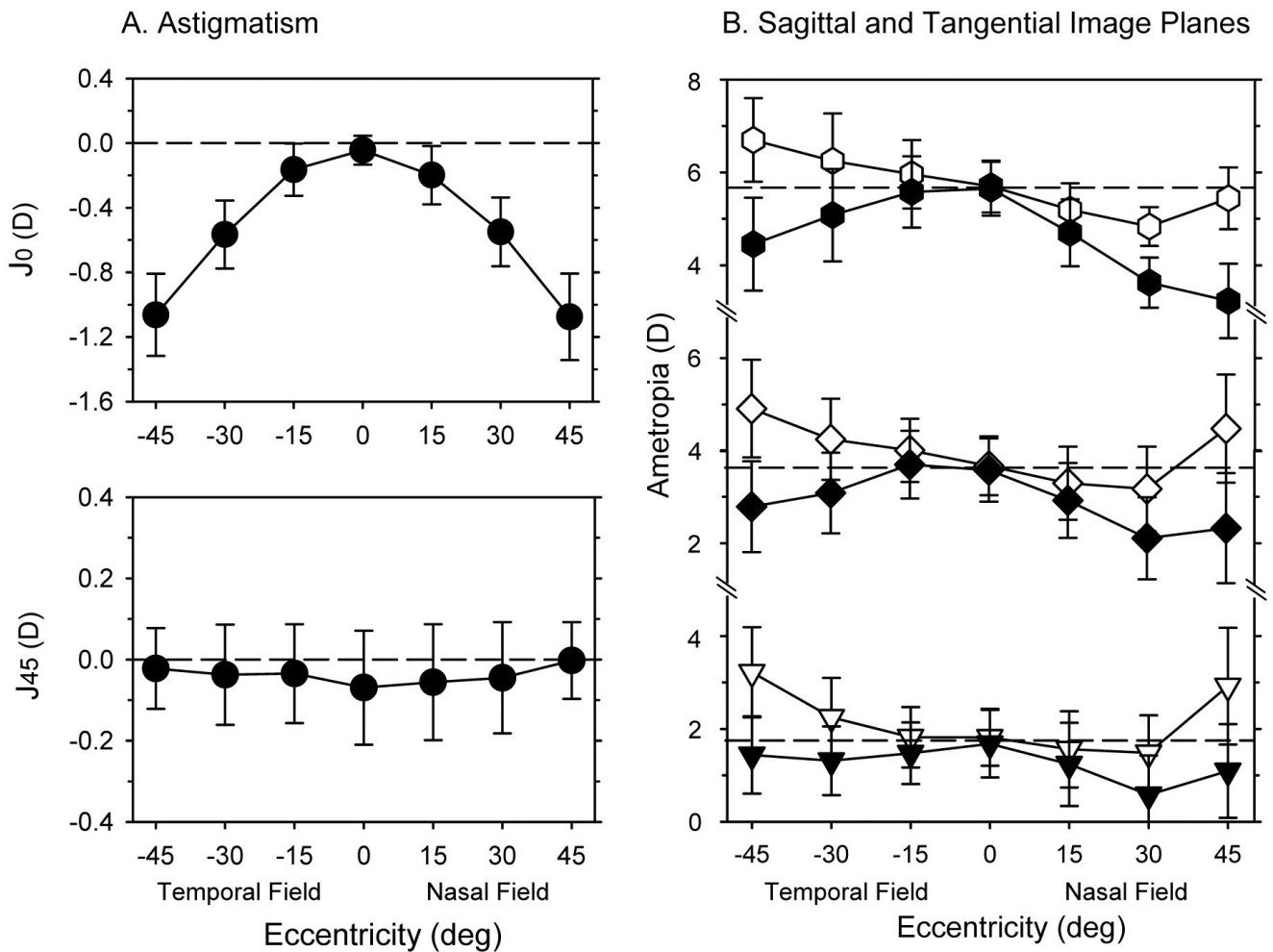


Figure 3. A. The average (\pm SD) amounts of astigmatism obtained along the horizontal meridian, expressed as the J_0 (upper) and J_{45} vector components (lower), plotted as a function of eccentricity for the right eyes of the 24-day-old infants. B. The average refractive errors (\pm SD) for the sagittal (open symbols) and tangential (filled symbols) astigmatic image planes plotted as function of horizontal eccentricity for the low, moderate and high hyperopic subgroups at 24 days of age. The dashed lines in each plot represent the average central refractive errors for each of the three subgroups.

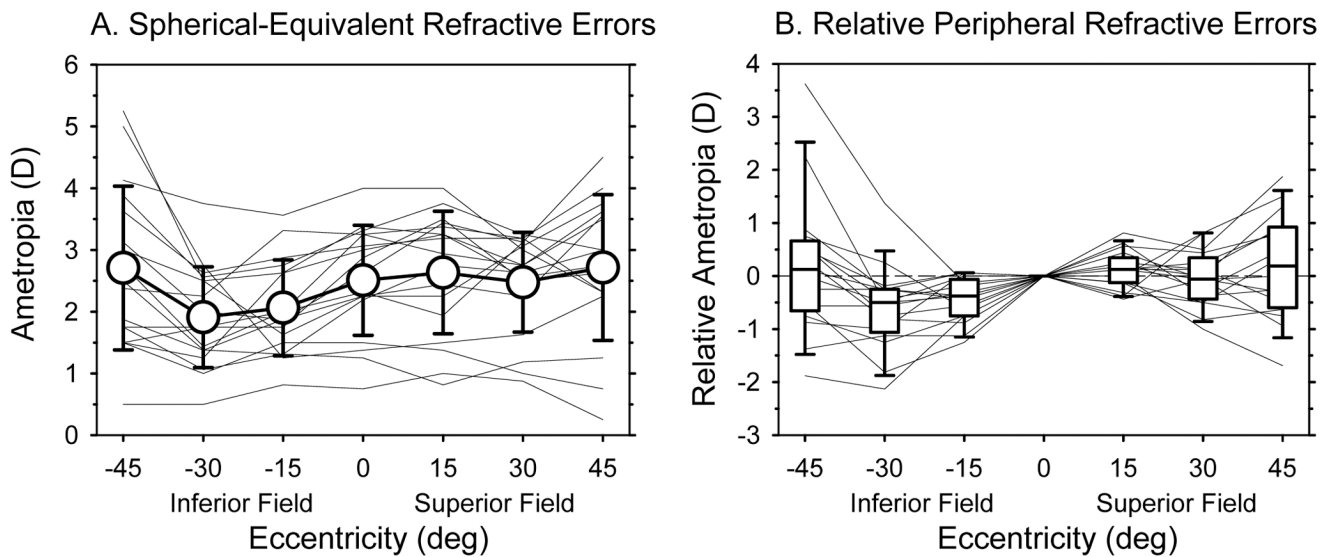


Figure 4.

A. Spherical-equivalent refractive errors plotted as a function of vertical eccentricity at 61 days of age for the 17 monkeys that were followed longitudinally. The thin lines represent the refractive errors for individual monkeys. The open circles represent the average refractive errors (\pm SD) at each eccentricity. B. Peripheral refractive errors for individual monkeys plotted relative their central refractive error as a function of vertical eccentricity. Thin lines represent individual monkeys. The lines in the box plots represent the medians. The boundaries of the box plots indicate the 25th and 75th percentiles. The error bars above and below the boxes indicate the 90th and 10th percentiles, respectively.

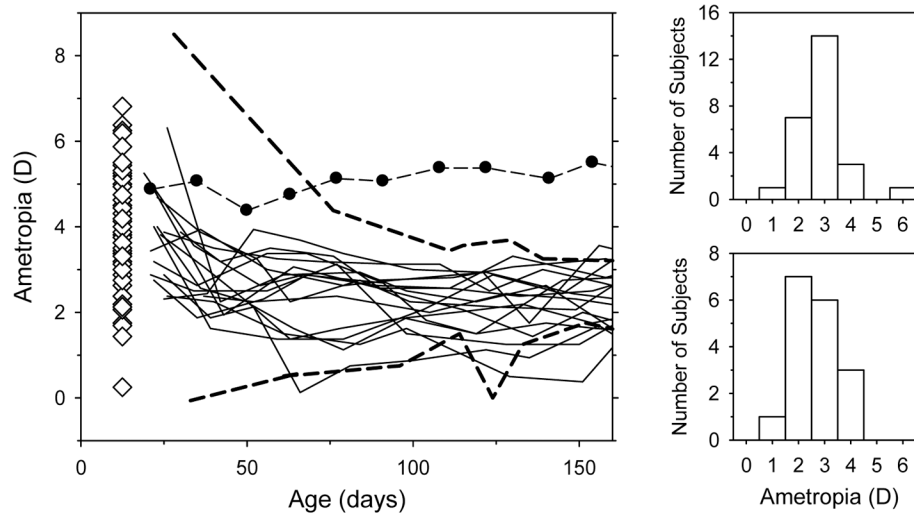


Figure 5.

Left. Spherical-equivalent refractive errors plotted as a function of age for the non-treated fellow eyes of the 13 experimental monkeys in the longitudinal subgroup (thin solid lines). For comparison, the dashed lines enclose the range of refractive errors obtained from 25 normal monkeys that were reared with unrestricted vision and that showed evidence of emmetropization. The filled symbols connected by dashed lines illustrate the refractive errors for an untreated monkey that, for unknown reasons, did not exhibit emmetropization. The open diamonds, which for clarity are plotted at 12.5 days of age, represent the right eye refractions for the 58 infants in the cross-sectional group obtained at 24 days of age. Right. Frequency distributions of refractive error (positive values indicate hyperopia) obtained at about 160 days of age for normal monkeys (upper) and for the non-treated fellow eyes of the 13 experimental monkeys (lower).

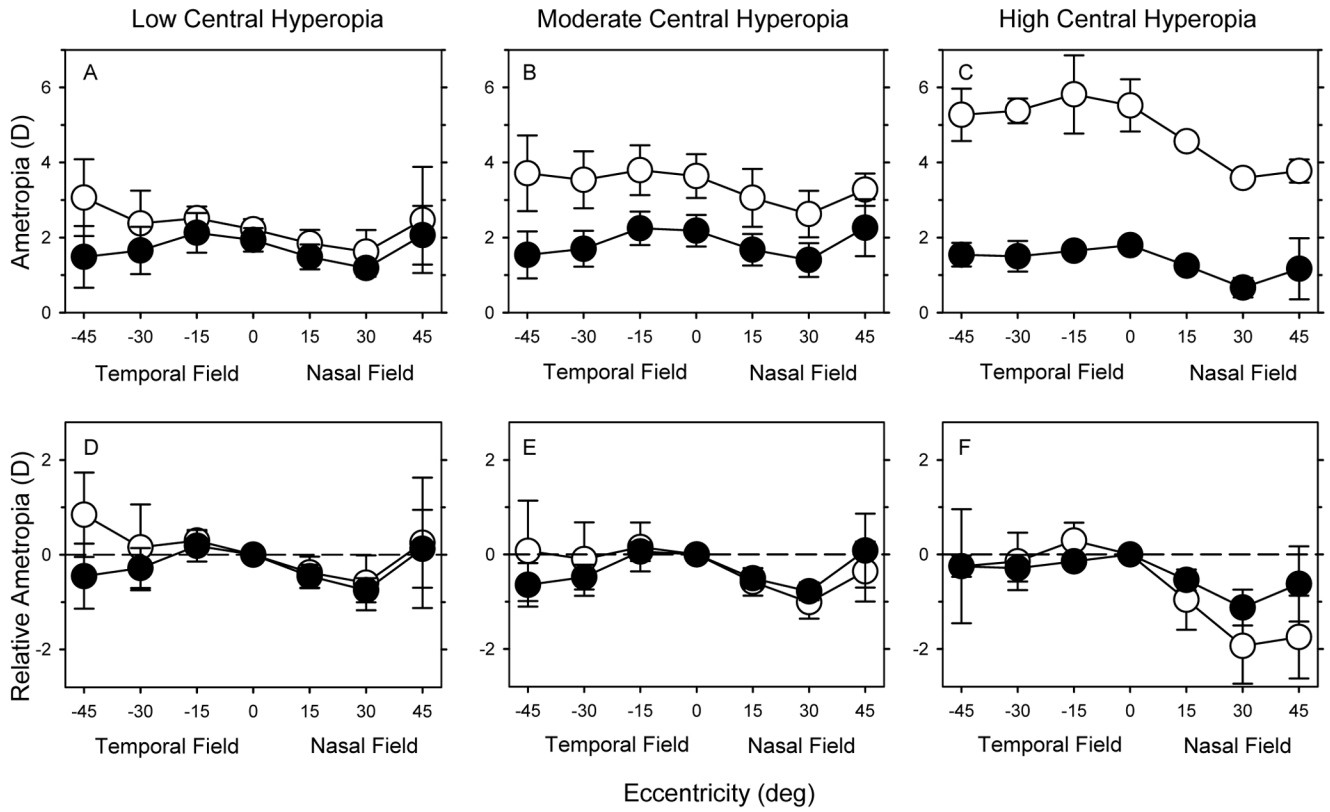


Figure 6. Spherical-equivalent refractive errors (\pm SD) (upper row) and relative peripheral refractive errors (lower row) plotted as a function of horizontal eccentricity for the low (left), moderate (middle) and high hyperopic subgroups (right). The open and filled circles represent data obtained at 24 and 308 days of age, respectively.

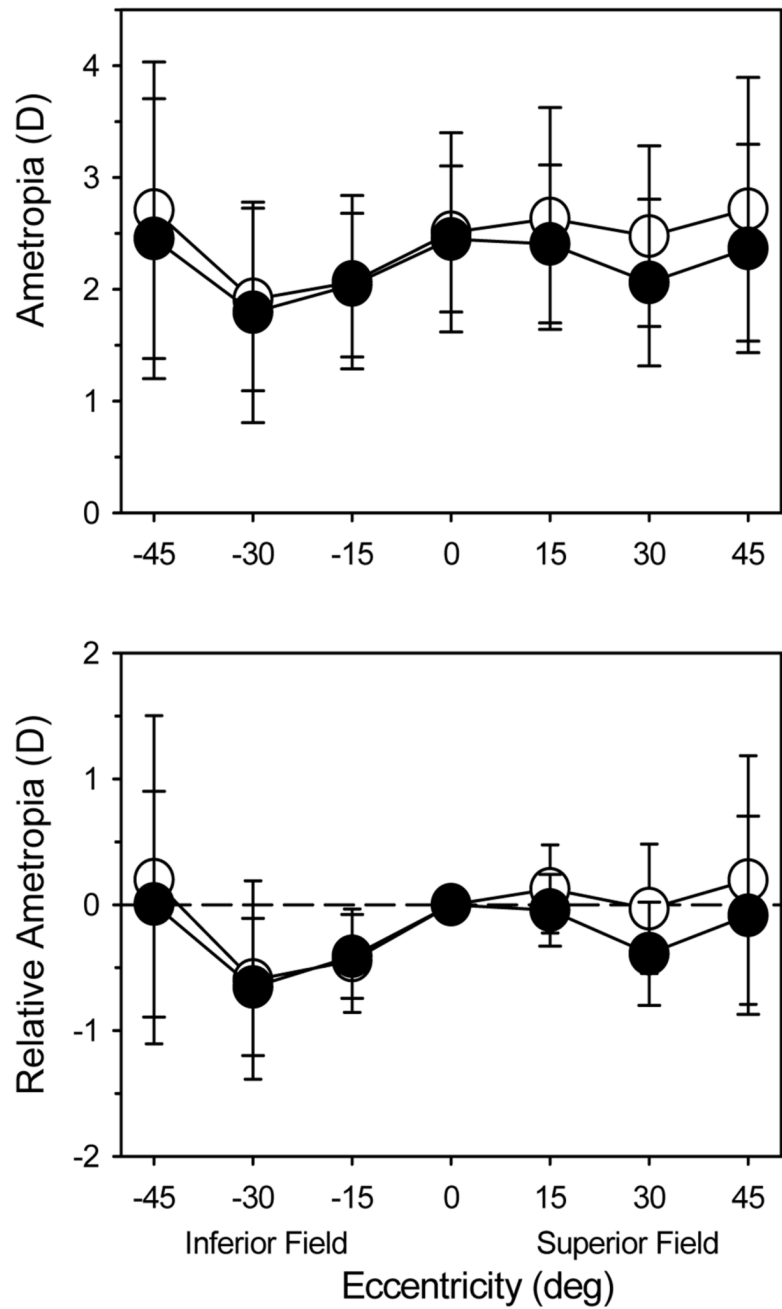


Figure 7. Average spherical-equivalent refractive errors (\pm SD, upper plot) and the average relative refractive error (\pm SD, lower plot) plotted as a function of vertical eccentricity for the monkeys that were followed longitudinally. The open and filled circles represent data obtained at 61 and 260 days of age, respectively.

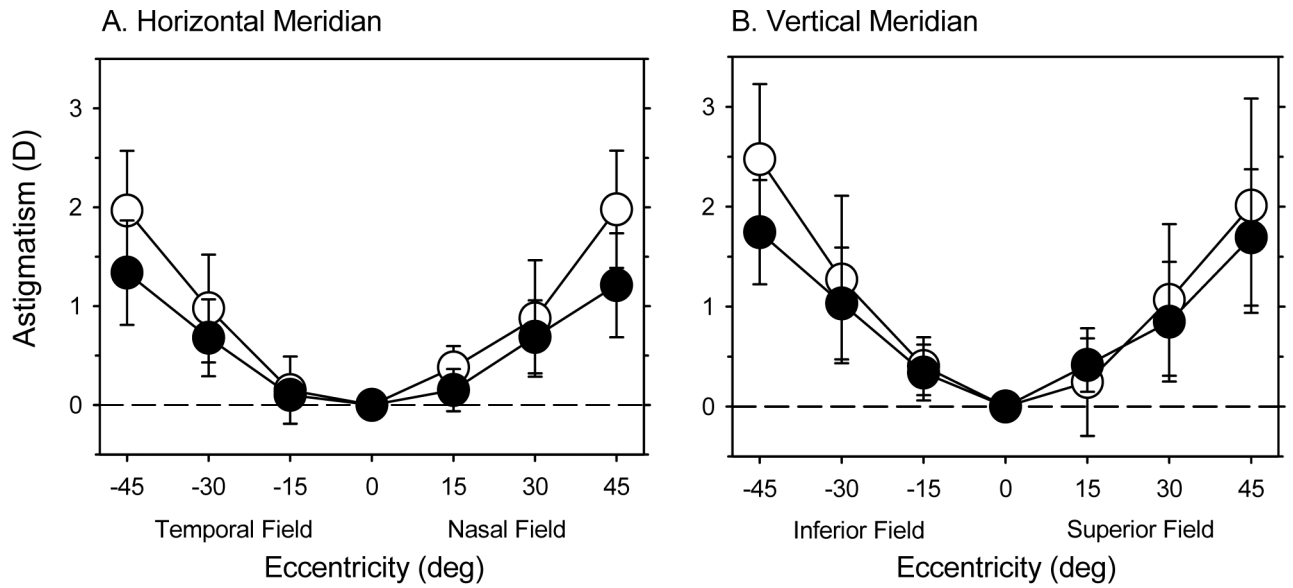


Figure 8.

The average amounts (\pm SD) of against-the-rule and with-the-rule astigmatism obtained in the horizontal (A) and vertical meridians (B), respectively. In A, the data represented by the open and filled symbols were obtained at 24 and 308 days of age, respectively. In B, the data represented by the open and filled symbols were obtained at 61 and 260 days of age, respectively.

Table 1

Relative peripheral refractive refractions at 308 days.

	45° Temporal Field (D)	30° Temporal Field (D)	15° Temporal Field (D)	15° Nasal Field (D)	30° Nasal Field (D)	45° Nasal Field (D)
High Hyperopes	-0.25 ± 0.23	-0.29 ± 0.28	-0.15 ± 0.10	-0.54 ± 0.22	-1.13 ± 0.38	-0.63 ± 0.80
Moderate Hyperopes	-0.64 ± 0.46	-0.48 ± 0.26	+0.06 ± 0.20	-0.51 ± 0.22	-0.44 ± 0.19	+0.44 ± 0.78
Low Hyperopes	-0.45 ± 0.69	-0.28 ± 0.42	+0.19 ± 0.33	-0.45 ± 0.24	-0.75 ± 0.26	+0.13 ± 0.82